Author Manuscript

Author Manuscript

Author Manuscript

Author Manuscript

HHS Public Access

Author manuscript

*Metallomics*. Author manuscript; available in PMC 2020 April 22.

Published in final edited form as:

*Metallomics*. 2019 July 17; 11(7): 1298–1309. doi:10.1039/c9mt00104b.

# Isolated *Saccharomyces cerevisiae* vacuoles contain low-molecular-mass transition-metal polyphosphate complexes†

**Trang Q. Nguyen**[a], **Nathaniel Dziuba**[b], **Paul A. Lindahl**[a,b]

[a]Department of Chemistry, Texas A&M University, College Station, TX 77843-3255, USA

[b]Department of Biochemistry and Biophysics, Texas A&M University, College Station, TX 77843, USA

## Abstract

Vacuoles play major roles in the trafficking, storage, and homeostasis of metal ions in fungi and plants. In this study, 29 batches of vacuoles were isolated from *Saccharomyces cerevisiae*. Flow-through solutions (FTS) obtained by passing vacuolar extracts through a 10 kDa cut-off membrane were characterized for metal content using an anaerobic liquid chromatography system interfaced to an online ICP-MS. Nearly all iron, zinc, and manganese ions in these solutions were present as low-molecular-mass (LMM) complexes. Metal-detected peaks with masses between 500–1700 Da dominated; phosphorus-detected peaks generally comigrated. The distribution of metal:polyphosphate complexes was dominated by particular chain-lengths rather than a broad binomial distribution. Similarly treated synthetic $Fe^{III}$ polyphosphate complexes showed similar peaks. Treatment with a phosphatase disrupted the LMM metal-bound species in vacuolar FTSs. These results indicated metal:polyphosphate complexes 6–20 phosphate units in length and coordinated by 1–3 metals on average per chain. The speciation of iron in FTSs from iron-deficient cells was qualitatively similar, but intensities were lower. Under healthy conditions, nearly all copper ions in vacuolar FTSs were present as 1–2 species with masses between 4800–7800 Da. The absence of these high-mass peaks in vacuolar FTS from *cup1Δ* cells suggests that they were due to metallothionein, Cup1. Disrupting copper homeostasis increased the amount of LMM copper:polyphosphate complexes in vacuoles (masses between 1500–1700 Da). Potentially dangerous LMM copper species in the cytosol of metallothionein-deficient cells may traffic into vacuoles for sequestration and detoxification.

†Electronic supplementary information (ESI) available: This includes: Table S1, batches of vacuoles isolated in this study; Fig. S1, calibration of the size-exclusion column; Fig. S2–S5, individual Fe-, P-, Zn-, and Mn-detected chromatograms of vacuolar FTSs; Fig. S6, overlays of Mn and P for Batch 13, 16, 17, and 18 at pH 8.5 mobile phase; Fig. S7, P-detected chromatograms of FTS from isolated vacuoles from WT strain in the presence of phosphatase inhibitors; Fig. S8, Cu-detected chromatograms of FTS from isolated vacuoles from WT strain; and Fig. S9, Cu-detected chromatograms of FTS from isolated vacuoles from *cox17Δ* and *cup1Δ* cells. See DOI: 10.1039/c9mt00104b

Lindahl@chem.tamu.edu; Fax: +1-979-845-4719; Tel: +1-979-845-0956.

Author contributions

P. A. L. and T. Q. N. designed the experiments. P. A. L. offered advice and wrote most of the paper. T. Q. N. conducted all of the experiments, analyzed data and prepared figures. N. M. D. maintained the LC-ICP-MS instrument, trained T. Q. N. on the instrument and obtained the LC calibration curve.

Conflicts of interest

There are no conflicts to declare.

Author Manuscript Author Manuscript Author Manuscript Author Manuscript

## Introduction

Vacuoles are acidocalcisome-like organelles found in fungi and plants.[1–4] These acidic structures are related to endosomes and lysosomes in humans, and are used in endocytosis, secretory trafficking, autophagy, and metabolite recycling. Vacuoles in *S. cerevisiae* cells grown to stationary phase in media buffered at pH = 6 have a pH of 6.2.[5] The pH gradient with cytosol drives the import of metal ions into the organelle,[3] allowing vacuoles to store essential metals[1,6–11] and sequester toxic metal ions that would otherwise engage in deleterious cellular reactions.[12,13]

Iron fits in both of these categories; it is essential for cell growth and can generate reactive oxygen species *via* Fenton-based reactions.[14] Some cellular iron enters vacuoles through the Ccc1 protein located on the vacuolar membrane.[15,16] Some extracellular iron enters vacuoles through endocytosis.[15] Vesicular fluid-phase endocytic transport to and from vacuoles plays a major role in metal homeostasis.[17] Vacuoles concentrate nutrient metal ions in the environment for eventual delivery to the cytosol.

Iron in vacuoles can be mobilized and exported to the cytosol through specific iron-export proteins on the vacuolar membrane. These include the Fet5:Fth1 ferroxidase:permease complex[18] and the Nramp protein Smf3.[19,20] The ultimate concentration of vacuolar iron is controlled by opposing rates of iron import and export.

These organelles are oxidizing relative to the cytosol, and so iron is typically stored as $Fe^{III}$ rather than $Fe^{II}$.[9,20–23] EPR spectra of isolated vacuoles exhibit a $g = 4.3$ signal indicating high-spin $S = 5/2$ $Fe^{III}$ ions with rhombic symmetry. $Fe^{III}$ ions in vacuoles must be reduced to $Fe^{II}$ prior to export to the cytosol. This process is controlled by ferrireductase Fre6.

An important aspect of vacuolar metabolism involves polyphosphate (polyP) ions, linear polyanionic polymers of phosphate units linked by phosphoanhydride bonds.[24] WT yeast cells contain 25–42 mM orthophosphate ($P_i$) and 23–250 mM polyP (concentration given in terms of phosphate units).[6,25] Most polyP ions are located in vacuoles.[26]

Preassembled polyP chains cannot be imported into vacuoles.[3] Rather they must be synthesized on the vacuolar membrane and inserted ratchet-like into the lumen.[3,26,27] Once in the lumen, polyP chains can be hydrolyzed by vacuolar phosphatases Ppn1 and Ppn2.[28] Ppn1 has both exopolyphosphatase and endopolyphosphatase activities. Activity requires manganese or magnesium ions.[26] Ppn2 is exclusively an endophosphatase that is activated by zinc.[29] Both enzymes are delivered to the vacuole *via* the multi-vesicular body pathway in which proteins are packaged into luminal vesicles that fuse with vacuoles and release their contents.[30,31]

The length of polyP chains (defined in terms of residues $n$) depends on the carbon and nitrogen source in the growth medium, as well as on metal ion availability.[5,32–34] Reported values of n include 7, 15, 20, and 60–100.[5,17,33,37] In the presence of high concentrations of metals, $n$ reportedly increases to 45–75, ~200, and >300.[3,17,34] Each internal $P_i$ residue has a mass of 79 Da; thus, polyP chains with $n = 7–100$ units have masses between 600–8000 Da.

Author Manuscript Author Manuscript Author Manuscript Author Manuscript

The high concentration of polyP in vacuoles and the strong binding of $Fe^{III}$ to polyP chains[35,36] led Raguzzi *et al.* to hypothesize that $Fe^{III}$ ions must be coordinated to polyP in vacuoles.[9] Supporting this, Mössbauer spectra of intact vacuoles reveal high-spin $S = 5/2$ $Fe^{III}$ ions whose spectra can be simulated using parameters expected for coordination to hard-oxygen ligands like polyP.[21,22] Moreover, spectra of authentic $Fe^{III}$ polyP in acidic pH are nearly indistinguishable from those of intact vacuoles. $Fe^{III}$ oxyhydroxide nanoparticles form when $Fe^{III}$ polyP solutions are adjusted to high pH similar to those observed spectroscopically in some batches of isolated vacuoles.[21,22]

Vacuoles are also involved in the trafficking, storage, and regulation of other metal ions such as zinc, manganese, and copper.[1,6,8,10,11,36] Importers and exporters for zinc and manganese are known. Copper enters vacuoles through an unknown mechanism but exits *via* membrane-bound Ctr2.[37,38] Copper is thought to be stored as $Cu^{II}$ ions in vacuoles, and then reduced to $Cu^{I}$ by Fre6 prior to export.[20,38,39]

Here, we have detected and partially characterized low-molecular-mass (LMM) iron, zinc, manganese and copper complexes from isolated vacuoles using a liquid chromatography system located in a refrigerated anaerobic glove box and interfaced with an online inductively coupled plasma mass spectrometer. Using this LC-ICP-MS system, we provide new additional evidence that most of these metal species in vacuoles are indeed present as metal–polyP complexes, with particular chain lengths dominating. Under healthy conditions, most copper ions in vacuolar extracts were present as high-molecular-mass (HMM) species (primarily or exclusively bound to metallothionein, Cup1) whereas in cells lacking Cup1, significant amounts of copper ions were coordinated to polyP chains. Implications of these results for cellular metal metabolism are discussed.

## Experimental procedures

### Cell growth

*Saccharomyces cerevisiae* strains W303 WT (MATα, *ura3-1, ade2-1, trp1-1, his3-11, 15, leu2-3, 112; ATCC*), *cup1Δ* (MATα, *trpl-1, gal-1, met13, can1, cup1S, ura3-50, Ade*$^{-}$ *His*$^{-}$ *cup1Δ::ura3*), and *cox17Δ* (Mat-a, *his3Δ1, leu2Δ0, met15Δ0, ura3Δ0, cox17::HphMX4*) were used in this study. The background for *cup1Δ* cells was MATα, *trpl-1, gal-1, met13, can1, cup1S, ura3-50, Ade*$^{-}$ *His*$^{-}$ whereas that for *cox17Δ* cells was BY4741. WT cells were typically grown in 500 mL of either complete synthetic medium (CSM) or minimal medium (MM). *cup1Δ* and *cox17Δ* cells were grown in 1 L of CSM. The composition for MM included 2% (w/v) glucose, 0.5% (w/v) ammonium sulfate, 0.17% (w/v) modified YNB lacking copper and iron (MP Bio), 20 mg $L^{-1}$ uracil, 20 mg $L^{-1}$ histidine, 50 mg $L^{-1}$ tryptophan, 100 mg $L^{-1}$ adenine, and 100 mg $L^{-1}$ leucine. CSM composition is similar to MM with the exceptions of using 6% (w/v) glucose and replacing most of the specific amino acids with the Yeast Synthetic Drop-out Medium Supplements (Y1376, Sigma-Aldrich). The growth medium was typically supplemented with 10 μM $CuSO_4$ and either 1 or 40 μM $^{56}Fe^{III}$ citrate. Starting with a single colony on YPAD plates, 50 mL (for WT strain) or 100 mL (for *cup1Δ* and *cox17Δ* strains) of precultures were grown in either CSM or MM at 30 °C for 24–48 hours. Cells were then inoculated into either 500 mL or 1 L of CSM or MM in a 2.8 L baffle flask and grown at 30 °C and 130 rpm. WT cells were harvested either at mid-

Author Manuscript Author Manuscript Author Manuscript Author Manuscript

exponential phase ($OD_{600}$ = 0.8 ± 0.1 for MM) or early stationary phase ($OD_{600}$ = 3.0 ± 0.1 for MM and $OD_{600}$ = 8.5 ± 0.1 for CSM). *cup1Δ* and *cox17Δ* cells were harvested at $OD_{600}$ = 5 and 8, respectively. Typical yields were 13 ± 2 g of wet cell pellet. Additional conditions for individual batches are in Table S1 (ESI†).

## Isolation of vacuoles

Vacuoles were isolated using the protocol of Li *et al.*[15] with some modifications for large-scale batches. Harvested cells were washed (centrifuged at 4000 × *g* for 5 min, supernatant-disposed, and pellet resuspended) 3 times with 5 mL of Buffer A (1 mM EDTA, 1.2 M sorbitol, and 200 mM $KP_i$, pH = 7.4) per g wet-pellet, followed by 3 additional washes with DI water. Cells were suspended in 5 mL of Buffer B (5 mM TCEPS, 100 mM Tris, pH = 7.4) per g wet cell mass. After 30 min incubation at 30 °C, cells were centrifuged and resuspended in 10 mL of Buffer C (0.6 M sorbitol, 10 mM $KP_i$, pH = 7.4,) per g of wet cells. PMSF was added to a final concentration of 8 mM. In addition, 3 mg of 200 KU-lyticase (Sigma Aldrich) per g wet cells were dissolved in 1 mL of Buffer C, and quantitatively transferred to the cell suspension. The initial $OD_{600}$ (immediately after adding lyticase) was measured by mixing 10 μL of cell suspension with 990 μL of water. Once $OD_{600}$ was 10–20% of the initial value, the suspension was centrifuged at 2200 × *g* for 5 min. Spheroplasts were gently resuspended in 3.5 mL of prechilled 15% Ficoll in Buffer D (200 mM sorbitol, 20 mM PIPES, pH = 6.8), and transferred to a prechilled 16 × 102 mm polypropylene ultracentrifuge tube (Beckman Coulter). A suspension of diethylaminoethyl dextran (DEAE-Dextran, Sigma-Aldrich) was prepared fresh in Buffer D (1–4 mg solid per mL of Buffer D), and was added to the spheroplast suspension to a final concentration of 200 μg $mL^{-1}$. The suspension was incubated for 3 min on ice followed by 5 min at 30 °C. The resulting subcellular fractionate was chilled on ice and overlaid first with 3 mL of 8% Ficoll, then 4 mL of 4% Ficoll, and finally 0% Ficoll to fill the tube to within 5 mm of the top. All Ficoll solutions were prepared in Buffer D and kept on ice. After centrifugation at 110 000 × *g* for 90 min with Beckman Coulter SW 32 Ti rotor in an Optima L-90K Ultracentrifuge, the vacuoles were collected at the 0–4% Ficoll interphase with a plastic disposable pipet (trimmed at the orifice to ~3 mm OD).

## Western blotting

Protein concentrations were quantified by Pierce™ BCA Protein Assay Kit (Thermo Scientific™). Whole cells protein extract and vacuolar fractions were run on a NuPAGE™ 10% Bis–Tris protein gel (Invitrogen™). Separated proteins were transferred to PVDF membranes using a Trans-Blot transfer cell (Bio-Rad). Membranes were blocked with 5% milk dissolved in Tris-buffered saline with 0.1% Tween (TBST-milk) for 1 h at RT before incubating with primary antibodies overnight at 4 °C. All primary antibodies were prepared in TBST-milk at the following dilutions: 1 : 2000 of anti-CPY antibody for vacuole/late

†Electronic supplementary information (ESI) available: This includes: Table S1, batches of vacuoles isolated in this study; Fig. S1, calibration of the size-exclusion column; Fig. S2–S5, individual Fe-, P-, Zn-, and Mn-detected chromatograms of vacuolar FTSs; Fig. S6, overlays of Mn and P for Batch 13, 16, 17, and 18 at pH 8.5 mobile phase; Fig. S7, P-detected chromatograms of FTS from isolated vacuoles from WT strain in the presence of phosphatase inhibitors; Fig. S8, Cu-detected chromatograms of FTS from isolated vacuoles from WT strain; and Fig. S9, Cu-detected chromatograms of FTS from isolated vacuoles from *cox17Δ* and *cup1Δ* cells. See DOI: 10.1039/c9mt00104b

Author Manuscript Author Manuscript Author Manuscript Author Manuscript

endosome marker (Life Technologies, A-6428), 1 : 1000 of anti-ALP antibody for vacuole marker (Abcam, 1D3A10), 1: 2000 of anti-Kar2 antibody for endoplasmic reticulum marker (Santa Cruz Biotechnology, sc-33630), 1: 2000 of anti-PGK antibody for cytosol marker (Life Technologies, H0460) and 1 : 1000 of anti-porin antibody for mitochondria marker (Thermo Fisher, 16G9E6BC4). Goat anti-rabbit IgG HRP-conjugated secondary antibody was from Santa Cruz Biotechnology (clone sc-2004) and goat anti-mouse IgG HRP-conjugated secondary antibody was from Invitrogen (clone G-21040). Both secondary antibodies were used at 1 : 5000 dilution for 1 h at RT. Clarity™ Western ECL Substrate (Bio-Rad) was added, and images were obtained (FujiFilm LAS-4000 mini) with a 15 s exposure using the precision mode of chemiluminescence setting.

## Confocal microscopy

A 2-well Lab-Tek™ Chambered Borosilicate Coverglass (Fisher Scientific) was coated with 20 mL of 0.1% (w/v) poly-L-lysine solution (Sigma Aldrich) for 30 min and dried in air overnight. A stock solution of 10 mM green fluorescent Yeast Vacuole Membrane Marker MDY-64 dye (Fisher Scientific) was prepared by dissolving 1 mg of solid in 260 μL of DMSO. Aliquots (4 μL) were frozen in liquid $N_2$, stored at −20 °C in the dark. Freshly isolated vacuoles (20–50 μL) were gently mixed, affording a final dye concentration of 10 μM. The mixture was incubated at RT for 5 min. Fluorescent stained vacuoles were then applied to the coated coverglass. Vacuoles were imaged with a Zeiss LSM 780 confocal microscope at TAMU Department of Veterinary Integrative Biosciences using an excitation wavelength of 451 nm and emission wavelength of 497 nm.

## Preparation of $Fe^{III}$ polyphosphate

0.5 mg $mL^{-1}$ of sodium polyphosphate (Acros Organics) was prepared in Buffer D and passed through an Ultracel regenerated cellulose 10 kDa NMWL membrane (EMD Millipore) using an Amicon® EMD Millipore Stirred Cell (Model 8003, 3 mL). To 10 mL of the resulting flow-through solution (FTS) was added 270 mg of $FeCl_3.6H_2O$ (Sigma Aldrich). The resulting 100 mM $FeCl_3$ stock solution was serially diluted using polyP FTS to yield 5, 10, 25, and 50 μM of $FeCl_3$ in 0.5 mg $mL^{-1}$ PolyP.

## Preparation of vacuolar FTS and LC-ICP-MS chromatography

2–2.5 mL of isolated vacuolar extract (in Buffer C, obtained from the 0–4% Ficoll interface) were treated with 2% (v/v, final) Triton X-100 and passed through a 10 kDa cut-off membrane (EMD Millipore) using the stirred cell described above. Almost 90% of the vacuolar extract passed through the 10 kDa membrane in *ca.* 1 h. The FTS (150 or 500 μL) was loaded onto a dipeptide size-exclusion (SEC) Superdex™ Peptide 10/300 GL column (GE Life Sciences) connected to an Agilent 1260 Bioinert quaternary pump (G5611A). A flow rate of 0.35 mL $min^{-1}$ was used with the mobile phase of either 20 mM $(NH_4)HCO_3$, pH = 8.5 or 20 mM $(NH_4)$OAc, pH = 6.5. The SEC column was calibrated such that apparent molecular masses could be estimated from eluent volumes of standards (Fig. S1, ESI†). LC-ICP-MS parameters, column cleaning procedure, and molecular mass calibration have been described.[40]

Author Manuscript Author Manuscript Author Manuscript Author Manuscript

### Vacuolar FTS treatment with acid phosphatase

1.5 mg of lyophilized acid phosphatase powder (P1146–50UN, Sigma-Aldrich) was dissolved in 525 μL of DI water. Vacuolar FTSs from batches 13 and 14 were mixed with the resulting acid phosphatase solution in a 1 : 1 v/v ratio and incubated at 37 °C for 3 h. The resulting solution was injected onto the LC using a mobile phase with pH 8.5.

### Elemental analysis

Elemental concentrations were measured as described.[40] Briefly, vacuolar extract and vacuolar FTSs of 4 independent batches were separated into 50 μL quadruplicates using 15 mL polypropylene screw-top vials. 400 μL of trace-metal-grade 70% w/v nitric acid (Fisher Scientific) was added to each vial. Vials were sealed with caps and electrical tape, then incubated at 85 °C for *ca.* 15 h. Each replicate was diluted with 7.55 mL of high-purity trace-metal-free double-distilled-deionized water. Samples were analyzed using ICP-MS (Agilent 7700x) in He collision mode. ICP standards were prepared from customized stock solutions (Inorganic Ventures), 5% w/v final concentration of trace-metal-grade nitric acid, and double-distilled-deionized water to generate calibration curves for each element.

## Results

### Twenty nine batches of vacuoles were isolated (Table S1, ESI†)

After density-gradient ultracentrifugation, the organelle congregated at the 0–4% Ficoll interphase (Fig. 1A, arrow). Western blots of soluble extracts of whole cells and isolated vacuolar lysates from this interface revealed that the organelle was significantly purified (Fig. 1A) but also contaminated with endoplasmic reticulum (ER) and cytosol. No contamination from mitochondria was evident.

We evaluated the integrity of isolated vacuole batches using confocal fluorescence microscopy. Samples were treated with a fluorescent dye that localized to vacuolar membranes. Images revealed intact membranes (Fig. 1B). Vacuoles were distributed in size, ranging from 1–3 μm in diameter. Unidentified contaminating small punctate structures were also evident.

Due to the limited quantities, we did not determine absolute metal ion concentrations in isolated organelle batches. Rather, we determined the ratio of metal concentrations (nM) of vacuolar extracts and FTSs to the overall protein concentration (mg $mL^{-1}$) of the vacuolar extract ($[proteins]_{avg}$ = 0.5 ± 0.1 mg $mL^{-1}$, $n$ = 6). FTSs are the portion of soluble vacuolar extracts that passed through a 10 kDa cut-off membrane and contained LMM species. The average concentration-ratios of iron, zinc, copper and manganese in our FTSs and in soluble vacuolar extracts (Fig. 2) indicate that nearly all of the considered metal ions in vacuolar extracts are present as LMM complexes.

Ratios of [metal]/[protein] for Fe and Mn in vacuolar suspensions were similar to previous results,[21] especially for iron. The current [copper]/[protein] ratio was similar to the previous low-concentration group. The current [zinc]/[protein] ratio was 5-times lower than previous while the [phosphorus]/[protein] ratio was 3-times higher. Absolute concentrations in

Author Manuscript Author Manuscript Author Manuscript Author Manuscript

isolated vacuoles were previously determined to be: [$P_{vac}$] = 14 ± 9 mM; [$Fe_{vac}$] = 220 ± 100 μM; [$Zn_{vac}$] = 160 ± 120 μM; [$Cu_{vac}$] = 30 ± 30 μM (low group); [$Mn_{vac}$] = 1.7 ± 0.6 μM; [protein] = 6.3 mg $mL^{-1}$.[21] Some iron probably leached from vacuoles during isolation. Current P : Fe : Zn : Cu :Mn ratios were 10 : 1 : 0.12 : 0.11 : 0.02; previous ratios were 64 : 1 : 0.73 : 0.14 : 0.01.

## Iron-detected chromatograms of vacuolar FTS exhibit several LMM species

FTSs were passed down a size-exclusion chromatography column designed for optimal resolution of small peptides. We initially used a mobile phase of ammonium bicarbonate at pH 8.5 but later used ammonium acetate at pH 6.5. All of the elemental chromatograms of vacuolar FTS from WT cells are the average of individual traces that were categorized by the growth medium (complete synthetic media CSM *vs.* minimal media MM), growth phase at harvest (exponential *vs.* stationary phase), and the pH of the mobile phase. See Table S1 (ESI†) for all conditions. Individual chromatograms associated with Fig. S3, S4, S7–S10 are shown in ESI.†

Chromatography traces of FTSs from cells grown on MM and harvested in exponential and stationary phases exhibited three major iron-containing peaks with estimated masses of 1400, 1100, and 700 Da (Fig. 3, top 2 traces). We will refer to the species affording these peaks as $Fe_{1400}$, $Fe_{1100}$, and $Fe_{700}$. Masses were estimated from calibrated migration rates of known metal complexes and small metalloproteins under the same column conditions; we assume an uncertainty in mass of ±25%. Traces of FTSs from MM-grown cells harvested at stationary phase were more reproducible than those harvested during exponential phase, but major peaks were routinely in the same chromatographic region (700–1400 Da). More diverse peaks were observed using FTS from vacuoles isolated from cells grown on CSM and harvested during stationary phase (Fig. 3, middle 2 traces). The particular peaks observed depended on the pH of the mobile phase. At pH 8.5, major peaks were at 1700, 1400, 800, and 500 Da; at pH 6.5, they shifted to higher masses (2200, 1700, and 1200). Peaks of greater masses were evident in some traces. In summary, virtually all of the iron present in vacuolar extracts was present in LMM forms. These included *ca.* 8 LMM iron species, with apparent masses ranging from 2200–500 Da. There was some batch-to-batch variability, and species with higher masses were stabilized when the mobile phase of the chromatography column was slightly acidic.

Two batches were supplemented with 1 rather than 40 μM Fe in CSM. The speciation of iron in these batches was similar to that in batches grown with 40 μM iron; however, the intensities of the peaks were lower (Fig. 3, bottom 2 traces). This was almost certainly due to the lack of iron in vacuoles under nutrient iron-limited conditions. The intensity and position of zinc, manganese, and copper peaks from the same batches were similar to the corresponding peaks in iron-replete batches (see below), and they served as internal standards.

Author Manuscript Author Manuscript Author Manuscript Author Manuscript

## Phosphorus-detected chromatograms of FTS include phosphate and polyphosphate species

Vacuolar FTSs obtained from cells grown on CSM and harvested during stationary phase exhibited numerous phosphorus-detected chromatography peaks (Fig. 4). The dominant peak migrated in accordance with an apparent mass of 500 Da. This peak represented 90–95% of the overall phosphorus-based intensity in these chromatograms. Sodium phosphate eluted at the same elution volume (Fig. S3, ESI†). This was initially disconcerting since the mass of the $H_2PO_4^-$ ion is 97 Da, substantially lower than 500 Da. However, small highly charged ions migrate through standard Sephadex-based gel columns at rates that deviate from those expected, due to interactions between the mobile ions and the fixed charges within the column medium and/or due to the effects of different hydrodynamic volumes.[41] Based on these considerations, we tentatively assigned the 500 Da peak to a mixture of phosphate ions and short ($n$ = 6–8) PolyP chains.

Our primary interest was in the lower-intensity higher-mass phosphorus-based peaks. An expanded view of chromatograms of vacuolar FTS was obtained from cells grown on MM and using the LC column equilibrated at pH 8.5. This view revealed peaks at 1400, 1100, and 700 Da (Fig. 4). For cells grown on CSM, the equivalent chromatograms were similar but the main peak was shifted to 500 Da. Minor peaks at 2200 and 1700 Da are also evident. Using a mobile phase of pH 6.5, the peak at 1100 Da dominated the polyP region (Fig. 4, trace CSM-6.5).

We tentatively assigned all of these peaks to polyP chains. In many batches, unresolved low-intensity phosphorus-based absorption was also evident between 9000–1700 Da (Fig. S6, ESI†). This absorption, which is only evident by magnifying the plots and excluding the $P_{500/700}$ peaks, suggests that there is a low intensity broad statistical distribution of polyP chain lengths underlying higher-intensity peaks corresponding to particular polyP lengths.

We considered that some polyP chains hydrolyzed during isolation; this would explain the dominance of the 500 Da peak (as $P_i$). However, two batches isolated in the presence of phosphatase inhibitors cocktail did not yield significant changes in the intensities or elution volumes of our phosphorus-based chromatograms (Fig. S7, ESI†), suggesting that degradation during isolation was not a major problem.

## Evidence for iron:polyP complexes in vacuoles

Iron and phosphorus peaks comigrated in most batches. For example, using pH 8.5 mobile phase, iron and phosphorus peaks at 1700, 1400, 1100, and 500 Da comigrated. At pH 6.5, these same elements approximately comigrated at *ca.* 1200 Da. There were also unresolved minor phosphorus peaks in the region between 2200–1200 Da that comigrated with iron peaks. Iron and phosphorus peaks did not always comigrate, probably because the concentration of phosphorus was so much higher than the metal; thus the majority of observed polyP chains lacked iron and these would not comigrate.

Based on these results, we hypothesized that the comigrating peaks arose from $Fe^{III}$:polyP coordination complexes with masses between 1700–500 Da. One caveat was that with a mobile phase at pH 6.5, iron did not comigrate with the $P_i$ peak at 500 Da.

Author Manuscript Author Manuscript Author Manuscript Author Manuscript

The possibility that we were observing $Fe^{III}$:polyP complexes prompted us to prepare synthetic $Fe^{III}$ polyP complexes and examine their LC properties. Commercially purchased sodium polyP was incubated with $Fe^{III}Cl_3$ and passed through the 10 kDa cut-off membrane using the same procedure used to prepare vacuolar FTSs. Synthetic FTS was chromatographed as above, affording the traces shown in Fig. 5 which included iron peaks with approximate masses of 1400, 1200, and 900 Da. Phosphorus-based traces also showed peaks in this region, albeit not always perfectly comigrating. The experiment was performed three times with similar results within the displayed region. When $FeCl_3$ was injected onto the column in the absence of PolyP, only an iron-detected peak corresponding to a mass of 24 000 Da was observed (Fig. 5 inset). This peak was probably due to nanoparticle aggregates. Some of the added iron probably adsorbed onto the column and was not detected. A control sample of polyP alone also did not exhibit any Fe-detected peaks in the LMM region (Fig. 5). However, LC traces from polyP samples that had been incubated with $FeCl_3$ at increasing concentrations exhibited increasingly intense iron peaks between 1400–900 Da (Fig. 5). No peaks at or near 24 000 Da were present. Two other experiments showed similar results (data not shown). We tentatively conclude that the iron and phosphorus peaks observed here arose from particularly stable $Fe^{III}$ polyP complexes with apparent masses of 1400, 1200, and 900 Da. This supports our hypothesis that the comigrating Fe/P peaks observed in the same region of the chromatograms of the FTSs of vacuolar extracts arose from $Fe^{III}$:polyP complexes of similar composition. Complexes of particular masses were most evident in contrast to a broad binomial distribution of $Fe^{III}$:polyP complexes. The observed complexes must be either particularly stable or biosynthesized at higher levels.

If these peaks from vacuolar FTS arose from iron:polyP complexes, we reasoned that treating vacuolar FTS with acid phosphatase ought to disrupt the complexes. The control trace for such an experiment (prior to treatment) exhibited iron peaks at 1400, 700, and 500 Da and phosphorus peaks at 1400 and 500 Da (Fig. 6, Fe-pre and P-pre). Minor unresolved broad phosphorus-based peaks in the HMM region (*ca.* 5500 Da) were also observed. After treatment with acid phosphatase, the LMM iron peaks disappeared as iron peaks in the HMM void-volume region increased (Fig. 6, Fe-post). After treatment, the resulting phosphorus-detected trace exhibited an intense peak at 500 Da, stronger than in the control, and the peaks at 5500 Da and 1400 Da were gone (Fig. 6, P-post). We conclude that the FTS of vacuoles contain iron:polyP complexes with masses between 1400–500 Da, and that iron ions were released when the polyP chains were hydrolyzed by the phosphatase, generating $P_i$ that contributed at 500 Da. The released iron aggregated to exhibit the void peak in the Fe-post trace.

## Vacuoles also contains LMM zinc and manganese complexes

Zinc-detected chromatograms of vacuolar FTSs exhibited peaks at apparent masses between 1500–1200 Da (Fig. 7). $Zn_{1400}$ and $Zn_{1500}$ dominated when the mobile phase was pH 8.5 whereas $Zn_{1200}$ dominated at pH 6.5. Zinc peaks were generally more intense from batches that had been supplemented with zinc acetate in the growth medium (Fig. S4, ESI†). These peaks were also affected by phosphatase treatment (Fig. 6, Zn-pre *vs.* Zn-post) indicating that they also arose from zinc:polyP complexes. Most zinc ions eluted at the void volume after treatment, again suggesting aggregation. Curiously one peak ($Zn_{1400}$) remained after

Author Manuscript Author Manuscript Author Manuscript Author Manuscript

phosphatase treatment suggesting a different coordinating ligand. Zinc ions in vacuoles have been suggested to bind to glutamate and citrate.[42]

The corresponding manganese-detected traces showed more variability than other metals in terms of masses and intensities (Fig. 8). Most traces exhibited peaks between 1700–1300 Da but some exhibited peaks with masses between 9600–4700 Da. Using a mobile phase pH of 8.5, LMM species dominated (especially $Mn_{1400}$ for cells grown in MM, and $Mn_{1300}$ and $Mn_{1500}$ for cells grown on CSM). Using a mobile phase of pH 6.5, HMM species between 9600–4700 Da were evident. Broad low-intensity manganese and phosphorus absorption above 3000 Da were also evident (Fig. S6, ESI†). Assuming that this absorption reflects polyP chains of all possible lengths, manganese appears to bind randomly to this distribution (more so than other elements). Supplementing the growth medium with $MnCl_2$ had no noticeable effect on the intensities of the LMM Mn species. Mn peaks were also sensitive to phosphatase treatment (Fig. 6) suggesting that they (including the HMM species) arose from manganese:polyP complexes.

## Vacuolar FTS contains both HMM and LMM copper species

Copper-detected traces of FTS exhibited both high- and low-molecular mass features, with relative intensities affected by the growth medium. Chromatograms of vacuolar FTS from cells grown on MM (Fig. 9) contained a high-mass peak at *ca*. 7800 Da as well as a LMM peak at 1400 Da. $Cu_{1400}$ was absent in the CSM-based traces. Traces from cells grown on CSM were dominated by peaks with masses between 7800–4800 Da. Low-mass peaks between 1400–600 Da were generally present but of minor intensity relative to the higher-mass peaks. Using a mobile phase pH of 6.5, copper-detected traces of vacuolar FTS were dominated by two HMM copper species at 6400 and 4800 Da (Fig. 9), whereas at pH 8.5, the major species was at 7800 Da. $Cu_{7800}$ remained in vacuolar FTSs treated with acid phosphatase (Fig. 6, bottom panel), suggesting that this species is not polyP-based.

We considered that one or both of the HMM copper species with masses of 7800–4800 Da was either Cup1 or Cox17. Cup1 is a ~6600 Da cytosolic copper-storage metallothionein protein.[43] Cox17 is a ~7900 Da mitochondrial copper-binding protein that traffics copper to cytochrome *c* oxidase.[44] To examine these possibilities, we isolated vacuoles from *cup1Δ* and *cox17Δ* cells that had been grown on CSM and harvested during stationary phase. *cup1Δ* cells grew slower than normal and reached an $OD_{600}$ of only ~5 (WT cells typically reach an $OD_{600}$ of 7–8). The resulting chromatogram of the FTS from *cox17Δ* cells in one batch was devoid of $Cu_{7800}$ (Fig. 10, panel A). The equivalent chromatogram from another batch contained a peak at *ca*. 7800 Da but the intensity was less relative to vacuoles from WT cells. The results using vacuolar FTS from *cup1Δ* cells were more definitive, in that the HMM copper species observed in WT batches was absent in each of the four batches examined (Fig. 10, panel B). We conclude that the high-mass Cu peak is composed of Cup1. The deletion of Cox17 may exhibit pleiotropic effects that involve high-mass Cu peaks.

Relative to typical WT copper-based chromatograms, the FTS from *cup1Δ* and *cox17Δ* vacuoles contained more intense copper features in what we call the “true” LMM region (2000–500 Da) where proteins are unlikely to be coordinating ligands. The copper ions in

Author Manuscript Author Manuscript Author Manuscript Author Manuscript

this region appear to be coordinated to polyP chains as evidenced by comigrating phosphate-based species of similar masses (1700 and 1500 Da, see Fig. 10 green lines).

## Discussion

The vacuoles play major roles in the trafficking and homeostasis of metal ions in fungi and plants. This includes the dynamic storage and recycling of essential metal ions as well as the sequestration of what would otherwise be toxic metal ions. Despite these important roles, few mechanistic details are known regarding these processes. One reason is that vacuoles are difficult to purify, especially in the large quantities required for the biophysical, bioinorganic, and bioanalytical analyses that could tease-apart many of these details. In this study, we report a robust large-scale isolation method along with the first chromatographic characterization of the metal ions bound to polyphosphate in these organelles.

We first isolated vacuoles from cells grown exponentially on minimal media, but found that yields and reproducibility were better using cells grown on complete synthetic media and harvested in early stationary phase. Perhaps this is because vacuoles complete their biogenesis and morph into a single large structure during early stationary phase.[45] Even under these optimized conditions, we were unable to purify vacuoles completely; Western blot and confocal microscopic analyses showed some contamination of ER and cytosol – but not mitochondria. Thus, our batches should be viewed as highly enriched in vacuoles but with minor cytosol and ER contamination. The contamination was not a severe problem for our iron-related studies because most cellular iron is either in vacuoles or mitochondria; the iron concentrations in ER and cytosol are lower. ER and vacuoles are involved in the receptor-mediated sorting pathway of soluble vacuolar hydrolases.[46] As a result, it may not be possible to completely separate these two organelles. Due to these concerns and the lability of low-molecular-mass metal complexes, we decided to isolate a large number of batches and search for reproducible patterns. Rather than selecting one “representative” chromatogram for presentation, we present many traces and their averages to allow readers to assess for themselves the degree of reproducibility obtained. We regard this as laying the foundation for establishing the metal-related biochemistry associated with these delicate and intransigent organelles.

Our LC results provide the strongest evidence to date that most of the iron, zinc, and manganese ions (and some copper ions) in vacuoles are coordinated to polyP chains. Previous investigators used thermodynamic arguments based on the known strong coordination of these metal ions to polyP anionic chains in conjunction with the presence of high concentrations of iron and polyP in vacuoles to speculate that vacuoles contain such complexes. Previous studies from our lab focused on the spectroscopic properties of the iron in vacuoles which suggested the presence of $Fe^{III}$:polyP complexes. The behavior of vacuolar iron with variations of pH were also similar to those of authentic $Fe^{III}$:polyP complexes. The current study is the first to examine the metal and phosphorus content of isolated vacuoles using liquid chromatography.

Our results indicate that all of the four investigated metals in vacuoles are present in low-molecular-mass forms within vacuoles that migrate according to masses ranging from 10

Author Manuscript Author Manuscript Author Manuscript Author Manuscript

000–500 Da (see following scheme). Many (but not all) of the observed LC peaks comigrated with phosphorus, supporting the presence of metal:polyphosphate complexes in these organelles. Treatment with polyphosphatase disrupted these complexes, supporting this assignment. There were numerous instances in which the metals comigrated with each other, suggesting that multiple metals either bind to the same chain or to different chains of about the same length.

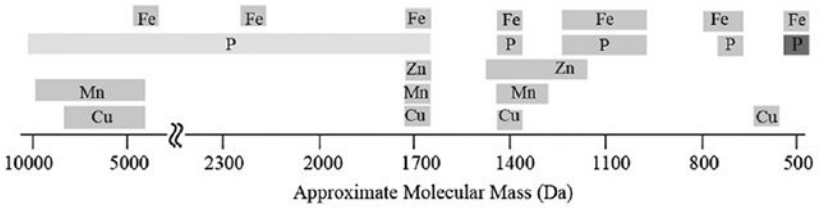


The length distribution of polyP chains in our samples was not primarily binomial. Rather, chains of 6–20 units long dominated, suggesting that these lengths were either especially stable or produced at especially high rates. We cannot explain these preferences but they must reflect the steady-state distribution resulting from opposing polyP synthesis and degradation processes. Metals may also preferentially bind to and/or stabilize chains of particular lengths *e.g.* due to chelation effects.

We calculated the molar ratio of phosphorus to iron, zinc, manganese and copper in the vacuolar FTS, and determined the percentage of each due to particular peaks in representative chromatograms. In most traces, the dominating $P_{500/700}$ peak represented 90–95% of the phosphorus in the sample. The LMM Fe species represented 80% of the iron in the sample. Thus, the P/Fe ratio for the LMM peaks should be roughly 10 : 1. This implies that one iron ion is coordinated, on average, to an $n = 10$ polyP chain. For a given polyP chain, one or two metal ions should be bound on average. The drawing in Fig. 11 represents a hypothetical metal-bound polyP chain.

Gerasimaite *et al.* reported that polyP was degraded during vacuolar isolation[31] and we considered that a similar phenomenon occurred here – *i.e.* a significant portion of the polyP may have hydrolyzed during our vacuolar isolation. However, our experiments in which phosphatase inhibitors were included during vacuolar isolation did not support this. Also, the masses of LMM metal:polyP species observed suggests polyP chain lengths in the same range as has been observed in previous studies. Trilisenko *et al.* reported an average polyP chain length (at pH 8.2) in isolated vacuoles of $5 \pm 2$.[47] They also found that 96% of phosphorus in isolated vacuoles was PolyP, with the remaining 4% present as $P_i$. The dominant phosphorus-detected peaks with approximate masses of 500–700 Da that we observe may arise from a mixture of short ($n = 6$–8) polyP chains and $P_i$.

Most copper ions in isolated vacuoles were present as 1–2 species with masses of 7800–4800 Da. These Cu peaks did not disappear after phosphatase treatment suggesting that they were not due to polyP complexes; we suspect that they are protein-bound and include Cup1. The situation may be different for the HMM manganese species, which migrated at the void volume after treatment with polyphosphatase. This suggests that high-mass manganese polyP complexes can form.

Author Manuscript Author Manuscript Author Manuscript Author Manuscript

Whether the detected Cup1 copper protein was present within vacuoles or in the cytosol contaminants of our batches is unknown. We favor the former possibility because the HMM copper species in our chromatograms were intense and present in nearly all batches; this is not the typical behavior of contaminants in which wide variations in peak intensities would be expected.

Few copper ions in vacuolar FTSs from WT cells grown on CSM medium were present as nonproteinaceous LMM species. However, the proportion of LMM copper increased significantly in samples from *cup1Δ* and *cox17Δ* cells; this proportion also was higher in WT cells grown on minimal medium. We hypothesize that dysregulation of copper homeostasis caused by the absence of Cup1 and Cox17 (or by growth of WT cells on minimal media) resulted in higher concentrations of aqueous copper ions, which were ultimately trafficked into vacuoles and bound to polyP for sequestration and detoxification. Gray and Jakob have suggested that the coordination of copper ions to polyP suppresses the tendency of copper to participate in Fenton-type reactions.[48] We hypothesize that the proportion of copper present as LMM nonproteinaceous species is either related to the degree of copper dysregulation or to a lack of copper chaperones or storage proteins.

Our major foci for this study were iron and copper speciation in vacuoles, but we also probed zinc and manganese. Under most conditions of this study, isolated vacuoles contained 8 times more iron than zinc and 50 times more iron than manganese. Although some batch-to-batch variations were observed, it is clear that most of the zinc and manganese ions coordinate to polyP chains. The majority of vacuolar LMM complexes of zinc and manganese were found to bind to polyP between 1400–1300 Da. One or more of these LMM zinc species may be used to metallate Pho8 alkaline phosphatase. Qiao *et al.* showed that metallating alkaline phosphatase Pho8 depended on vacuolar zinc importers Zrc1 and Cot1,[49] implying that vacuolar zinc is installed in apo-Pho8.

With this foundation laid, further advances in understanding the important role of these organelles in the cellular biology of metals should be forthcoming. We are interested in probing the redox properties of iron in vacuoles and exploring the trafficking of vacuolar iron to and from other cellular compartments including cytosol and mitochondria. The effect of nutrient phosphorus levels and the vacuolar polyphosphatases on the metal and polyP content of vacuoles might also be revealing. We attempted to isolate vacuoles under low $P_i$ medium to investigate the effect on the storage capabilities of transition metals. Unfortunately, our yields were insufficient for LC analysis. It may be useful to study vacuoles isolated from genetic strains in which vacuolar polyP levels are altered or in which another metallothionein (*CRS5*) is deleted.

## Supplementary Material

Refer to Web version on PubMed Central for supplementary material.

## Acknowledgements

We thank Dennis Thiele (Duke University School of Medicine) for the *cup1Δ* strain and helpful discussion, Vishal Gohil (TAMU Department of Biochemistry and Biophysics) for the *cox17Δ* strain, Charlie Baker and Natalie Garza

Author Manuscript Author Manuscript Author Manuscript Author Manuscript

from the Gohil lab for help with Western blots, and Roula Barhoumi Mouneimne (TAMU Department of Veterinary Integrative Biosciences) for assistance with the confocal microscopy. This work was supported by the National Institutes of Health (R35 GM127021), and the Robert A. Welch Foundation (A1170). The content is solely the responsibility of the authors and does not necessarily represent the official views of the National Institutes of Health or the Welch Foundation.

## Abbreviations

| | |
|---|---|
| **CSM** | Complete synthetic medium |
| **FTS** | Flow-through solution |
| **HMM** | High-molecular-mass |
| **LC** | Liquid chromatography |
| **LC-ICP-MS** | Liquid chromatography with on-line detection by an inductively coupled plasma mass spectrometer |
| **LMM** | Low-molecular-mass |
| **MM** | Minimal medium |
| **$P_i$** | Inorganic phosphate |
| **polyP** | Polyphosphate |
| **WT** | Wild-type |

## Notes and references

1. Docampo R, Ulrich P and Moreno SN, Evolution of acidocalcisomes and their role in polyphosphate storage and osmoregulation in eukaryotic microbes, Philos. Trans. R. Soc., B, 2010, 365, 775–784.
2. Blaby-Haas CE and Merchant SS, Lysosome-related Organelles as Mediators of Metal Homeostasis, J. Biol. Chem, 2014, 289, 28129–28136. [PubMed: 25160625]
3. Gerasimaite R, Sharma S, Desfougeres Y, Schmidt A and Mayer A, Coupled synthesis and translocation restrains polyphosphate to acidocalcisome-like vacuoles and prevents its toxicity, J. Cell Sci, 2014, 127, 5093–5104. [PubMed: 25315834]
4. Kane PM, Proton Transport and pH Control in Fungi, in Yeast Membrane Transport, ed. Ramos J, Sychrova H and Kschischo M, Advances in Experimental Medicine and Biology, 2016, vol. 892, pp. 33–68. [PubMed: 26721270]
5. Greenfield NJ, Hussian M and Lenard J, Effects of growth state and amines on cytoplasmic and vacuolar pH, phosphate, and polyphosphate levels in Saccharomyces cerevisiae: a $^{31}$P-nuclear magnetic resonance study, Biochim. Biophys. Acta, 1987, 926, 205–214. [PubMed: 3318934]
6. McNaughton RL, Reddi AR, Clement MHS, Sharma A, Barnese K, Rosenfeld L, Gralla EB, Valentine JS, Culotta VC and Hoffman BM, Probing in vivo $Mn^{2+}$ speciation and oxidative stress resistance in yeast cells with electron-nuclear double resonance spectroscopy, Proc. Natl. Acad. Sci. U. S. A, 2010, 107, 15335–15339. [PubMed: 20702768]
7. Bode HP, Dumschat M, Garotti S and Fuhrmann GF, Iron sequestration by the yeast vacuole: A study with vacuolar mutants of Saccharomyces cerevisiae, Eur. J. Biochem, 1995, 228, 337–342. [PubMed: 7705347]
8. Paidhungat M and Garrett S, Cdc1 and the vacuole coordinately regulate Mn2+ homeostasis in the yeast Saccharomyces cerevisiae, Genetics, 1998, 148, 1787–1798. [PubMed: 9560393]
9. Raguzzi F, Lesuisse E and Crichten RR, Iron Storage in Saccharomyces cerevisiae, FEBS Lett, 1988, 231, 253–258. [PubMed: 3282922]

Author Manuscript Author Manuscript Author Manuscript Author Manuscript


10. Okorokov LA, Lichko LP and Andreeva NA, Changes of ATP, polyphosphate and K+ contents in Saccharomyces carlsbergensis during uptake of $Mn^{2+}$ and glucose, Biochem. Int, 1983, 6, 481–488. [PubMed: 6679720]
11. White C and Gadd GM, The uptake and cellular distribution of zinc in Saccharomyces cerevisiae, J. Gen. Microbiol, 1987, 133, 727–737.
12. Ramsay LM and Gadd GM, Mutants of Saccharomyces cerevisiae defective in vacuolar function confirm a role for the vacuole in toxic metal ion detoxification, FEMS Microbiol. Lett, 1997, 152, 293–298. [PubMed: 9231423]
13. Nishimura K and Igarashi K, Proton gradient-driven nickel uptake by vacuolar membrane vesicles of Saccharomyces cerevisiae, J. Bacteriol, 1998, 180, 1962–1964. [PubMed: 9537401]
14. Bleackley MR, Young BP, Loewen CJR and MacGillivray RTA, High density array screening to identify the genetic requirements for transition metal tolerance in Saccharomyces cerevisiae, Metallomics, 2011, 3, 195–205. [PubMed: 21212869]
15. Li L, Chen OS, McVey Ward D and Kaplan J, CCC1 is a transporter that mediates vacuolar iron storage in yeast, J. Biol. Chem, 2001, 276, 29515–29519. [PubMed: 11390404]
16. Pimentel C, Vicente C, Menezes RA, Caetano S, Carreta L and Rodrigues-Pousada C, The role of the Yap5 transcriptional factor in remodeling gene expression in response to Fe bioavailability, PLoS One, 2012, 7, e37434. [PubMed: 22616008]
17. Klompmaker SH, Kohl K, Fasel N and Mayer A, Magnesium uptake by connecting fluid-phase endocytosis to an intracellular inorganic cation filter, Nat. Commun, 2017, 8, 1879, DOI: 10.1038/s41467-017-01930-5. [PubMed: 29192218]
18. Urbanoswski JL and Piper RC, The iron transporter Fth1p forms a complex with Fet5 iron oxidase and resides on the vacuolar membrane, J. Biol. Chem, 1999, 274, 38061–38070. [PubMed: 10608875]
19. Portnoy ME, Liu XF and Culotta VC, Saccharomyces cerevisiae expresses three functionally distinct homologues of the nramp family of metal transporters, Mol. Cell. Biol, 2000, 20, 7893–7902. [PubMed: 11027260]
20. Singh A, Kaur N and Kosman DJ, The metalloreductase Fre6p in Fe-efflux from the yeast vacuole, J. Biol. Chem, 2007, 282, 28619–28626. [PubMed: 17681937]
21. Cockrell AL, Holmes-Hampton GP, McCormick SP, Chakrabarti M and Lindahl PA, Mössbauer and EPR Study of Iron in Vacuoles from Fermenting Saccharomyces cerevisiae, Biochemistry, 2011, 50, 10275–10283. [PubMed: 22047049]
22. Cockrell AL, McCormick SP, Moore MJ, Chakrabarti M and Lindahl PA, Mössbauer, EPR, and Modeling Study of Iron Trafficking and Regulation in ΔCCC1 and Ccc1pup *Saccharomyces cerevisiae*, Biochemistry, 2014, 53, 2926–2940. [PubMed: 24785783]
23. Park J, McCormick SP, Cockrell A, Chakrabarti M and Lindahl PA, High-spin ferric ions in Saccharomyces cerevisiae vacuoles are reduced to the ferrous state during adenine-precursor detoxification, Biochemistry, 2014, 53, 3940–3951. [PubMed: 24919141]
24. Secco D, Wang C, Shou H and Whelan J, Phosphate homeostasis in the yeast Saccharomyces cerevisiae, the key role of the SPX domain-containing proteins, FEBS Lett, 2012, 586, 289–295. [PubMed: 22285489]
25. Auesukaree C, Homma T, Tochio H, Shirakawa M, Kaneko Y and Harashima S, Intracellular phosphate serves as a signal for the regulation of the PHO pathway in Saccharomyces cerevisiae, J. Biol. Chem, 2004, 279, 17289–17294. [PubMed: 14966138]
26. Gerasimaite R and Mayer A, Enzymes of yeast polyphosphate metabolism: structure, enzymology and biological roles, Biochem. Soc. Trans, 2016, 44, 234–239. [PubMed: 26862210]
27. Hothorn M, Neumann H, Lenherr ED, Wehner M, Rybin V, Hassa PO, Uttenweiler A, Reinhardt M, Schmidt A, Seiler J, Ladurner AG, Herrmann C, Scheffzek K and Mayer A, Catalytic Core of a Membrane-Associated Eukaryotic Polyphosphate Polymerase, Science, 2009, 324, 513–516. [PubMed: 19390046]
28. Sethuraman A, Rao NN and Kornberg A, The endopolyphosphatase gene: essential in Saccharomyces cerevisiae, Proc. Natl. Acad. Sci. U. S. A, 2001, 98, 8542–8547. [PubMed: 11447286]

Author Manuscript Author Manuscript Author Manuscript Author Manuscript


29. Breitkreutz A, Choi H, Sharom JR, Boucher L, Neduva V, Larsen B, Lin ZY, Breitkreutz BJ, Stark C, Liu G, Ahn J, Dewar-Darch D, Reguly T, Tang XJ, Almeida R, Qin ZS, Pawson T, Gingras AC, Nesvizhskii AI and Tyers M, A Global Protein Kinase and Phosphatase Interaction Network in Yeast, Science, 2010, 328, 1043–1046. [PubMed: 20489023]
30. Hurley JH and Emr SD, The ESCRT complexes: structure and mechanism of a membrane-trafficking network, Annu. Rev. Biophys. Biomol. Struct, 2006, 35, 277–298. [PubMed: 16689637]
31. Gerasimaite R and Mayer A, Ppn2, a novel $Zn^{2+}$-dependent polyphosphatase in the acidocalcisome-like yeast vacuole, J. Cell Sci, 2017, 130, 1625–1636. [PubMed: 28302909]
32. Vagabov VM, Trilisenko LV, Kulakovskaya TV and Kulaev IS, Effect of carbon source on polyphosphate accumulation in Saccharomyces cerevisiae, FEMS Yeast Res, 2008, 8, 877–882. [PubMed: 18647178]
33. Andreeva N, Ryazanova L, Dmitriev V, Kulakovaskaay T and Kulaev I, Adaptation of Saccharomyces cerevisiae to toxic manganese concentration triggers changes in inorganic polyphosphates, FEMS Yeast Res, 2013, 13, 463–470. [PubMed: 23663411]
34. Breus NA, Ryazanova LP, Dmitriev VV, Kulakovskaya TV and Kulaev IS, Accumulation of phosphate and polyphosphate by Cryptococcus humicola and Saccharomyces cerevisiae in the absence of nitrogen, FEMS Yeast Res, 2012, 12, 617–624. [PubMed: 22591314]
35. Van Wazer JR and Callis CF, Metal complexing by phosphates, Chem. Rev, 1958, 58, 1011–1046.
36. Kulaev IS, Vagabov VM and Kulakovskaya TV, The Biochemistry of inorganic polyphosphates, Wiley, Chichester, 2004.
37. Rees EM, Lee J and Thiele DJ, Mobilization of intracellular copper stores by the ctr2 vacuolar copper transporter, J. Biol. Chem, 2004, 279, 54221–54229. [PubMed: 15494390]
38. Rees EM and Thiele DJ, Identification of a vacuole-associated metalloreductase and its role in Ctr2-mediated intracellular copper mobilization, J. Biol. Chem, 2007, 282, 21629–21638. [PubMed: 17553781]
39. Kosman DJ, Molecular mechanisms of iron uptake in fungi, Mol. Microbiol, 2003, 47, 1185–1197. [PubMed: 12603727]
40. Dziuba N, Hardy J and Lindahl PA, Low-molecular-mass iron in healthy blood plasma is not predominately ferric citrate, Metallomics, 2018, 10, 802–817. [PubMed: 29808889]
41. Neddermeyer PA and Rogers LB, Gel filtration behavior of inorganic salts, Anal. Chem, 1968, 40, 755–762.
42. Kitamoto KK, Yoshizawa Y, Ohsumi Y and Anraku Y, Dynamic aspects of vacuolar and cytosolic amino acid pools of Saccharomyces cerevisiae, J. Bacteriol, 1988, 170, 2683–2686. [PubMed: 3131304]
43. Winge DR, Nielson KB, Gray WR and Hamer DH, Yeast metallothionein: sequence and metal binding properties, J. Biol. Chem, 1985, 260, 14464–14470. [PubMed: 3902832]
44. Abajian C, Yatsunyk LA, Ramirez BE and Rosenzweig AC, Yeast Cox17 solution structure and copper(I) binding, J. Biol. Chem, 2004, 279, 53584–53592. [PubMed: 15465825]
45. Conradt B, Shaw J, Vida T, Emr S and Wickner W, In vitro reactions of vacuole inheritance in Saccharomyces cerevisiae, J. Cell Biol, 1992, 119, 1469–1479. [PubMed: 1334958]
46. Bryant NJ and Stevens TJ, VacuoleBiogenesis inSaccharomyces cerevisiae: Protein transport pathways to the yeast vacuole, Microbiol. Mol. Biol. Rev, 1998, 62, 230–247. [PubMed: 9529893]
47. Trilisenko LV, Vagabov VM and Kulaev IS, The content and chain length of polyphosphates from vacuoles of Saccharomyces cerevisiae VKM Y-1173, Biochemistry, 2002, 67, 592–596. [PubMed: 12059781]
48. Gray MJ and Jakob U, Oxidative stress protection by polyphosphate – new roles for an old player, Curr. Opin. Microbiol, 2015, 24, 1–6. [PubMed: 25589044]
49. Kizawa K, Aono T and Ohtomo R, PHO8 gene coding alkaline phosphatase of Saccharomyces cerevisiae is involved in polyphosphate metabolism, J. Gen. Appl. Microbiol, 2016, 62, 297–302. [PubMed: 27829585]

Author Manuscript Author Manuscript Author Manuscript Author Manuscript

## Significance to metallomics

Vacuoles are organelles in fungi and plants that store and sequester metals for trafficking and detoxification. Liquid chromatography with on-line ICP-MS was used to show that nearly all Fe, Cu, Zn, and Mn in vacuoles are present as low-molecular-mass (< 10 kDa) polyphosphate complexes. Lengths between 6–27 phosphate units (500–2200 Da) dominated. In WT vacuoles, 1–2 Cu peaks were present with masses 4800–7800 Da; these were due primarily or exclusively to Cup1 metallothionein. Under conditions of copper dyshomeostasis, copper:polyphosphate complexes with masses 1700–1400 Da were generated, suggesting that toxic Cu ions became sequestered into vacuoles.

Author Manuscript Author Manuscript Author Manuscript Author Manuscript

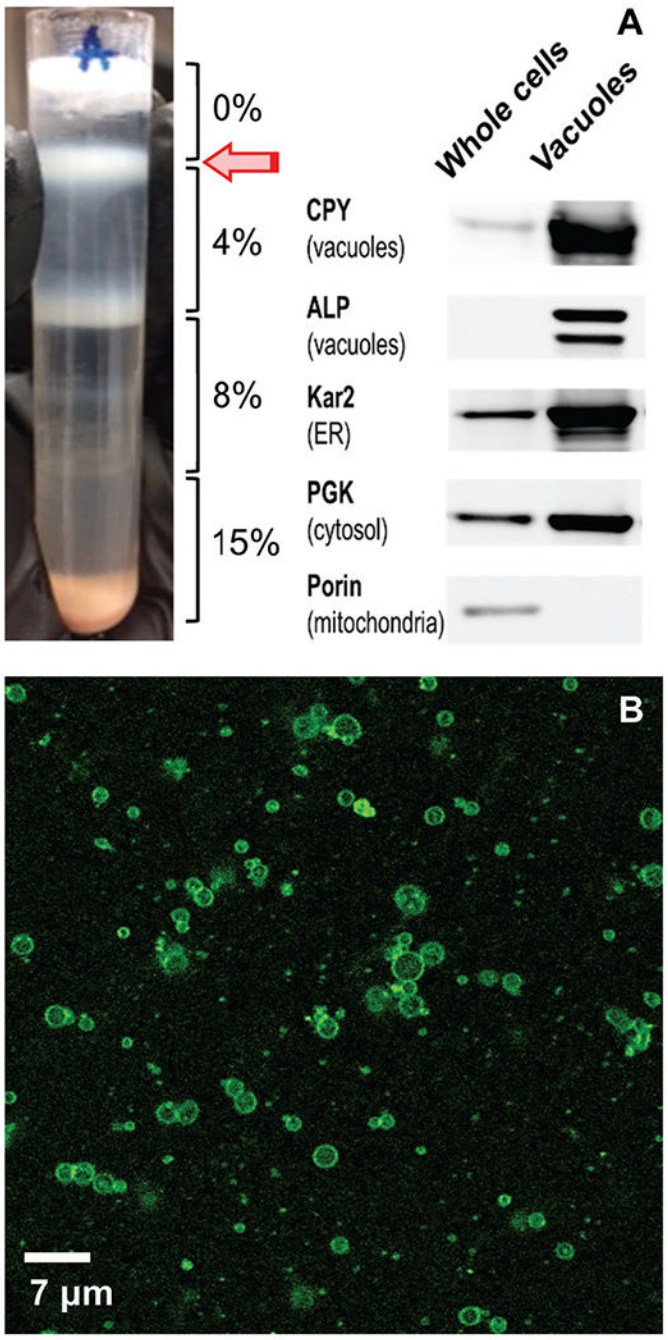


**Fig. 1.**

Purity and integrity of isolated vacuoles: (A) centrifugation tube after density gradient step of the isolation procedure. The white band at the 0%:4% Ficoll interface (arrow) was collected and called the isolated vacuole fraction. A Western blot of whole cells and the corresponding isolated vacuolar fraction is shown; 8 µg proteins were loaded each lane ($n$ = 2). (B) Confocal microscopic image of isolated vacuolar fraction ($n$ = 2).

Author Manuscript Author Manuscript Author Manuscript Author Manuscript

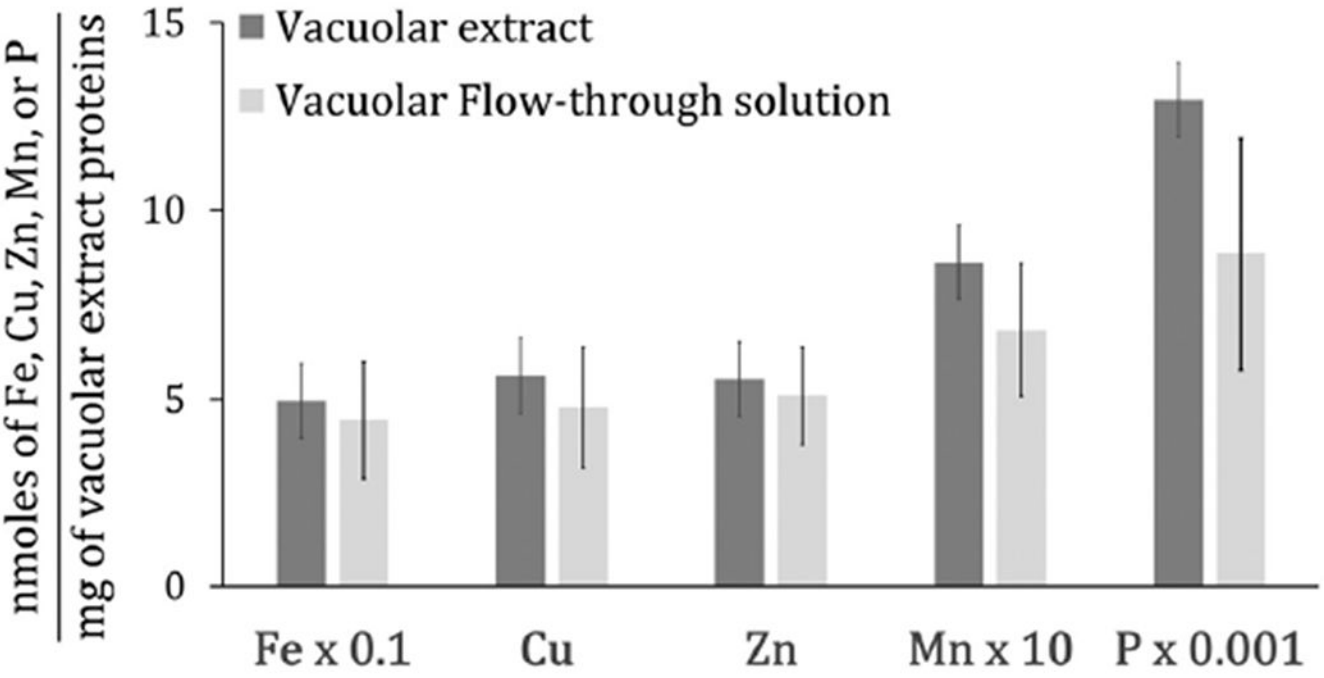


**Fig. 2.**
Histogram of elemental concentrations in vacuolar extracts and FTSs ($n = 4$).

Author Manuscript Author Manuscript Author Manuscript Author Manuscript

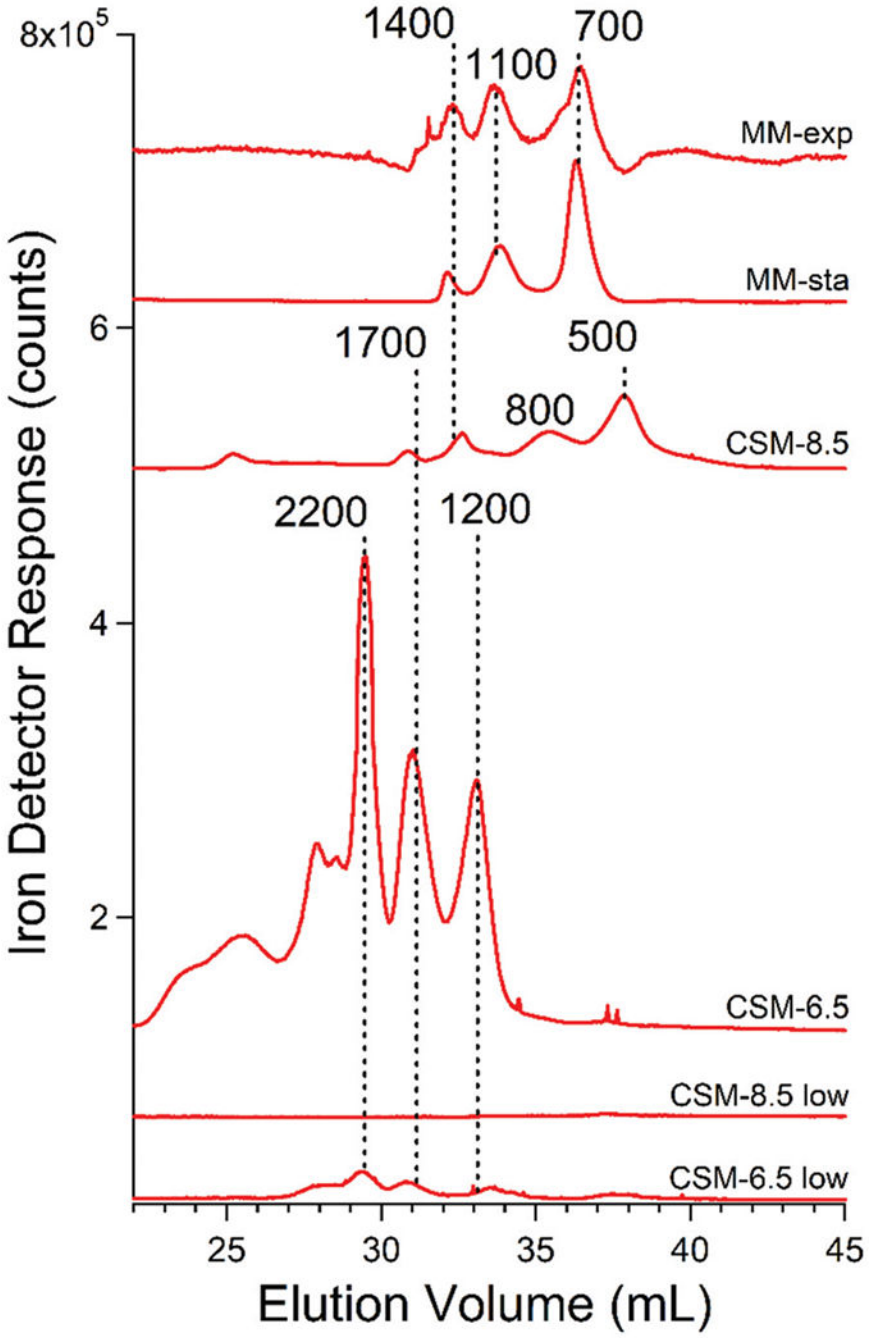


**Fig. 3.**

Averaged iron-detected chromatograms of FTS fromisolated vacuoles. *MM-exp*, average of traces obtained from MM-grown cells harvested under exponential conditions; *MM-sta*, average of traces obtained from MM-grown cells harvested under stationary conditions; *CSM-8.5*, averages of traces from CSM-grown cells using pH 8.5 mobile phase. *CSM-8.5 low*, same but for cells grown on 1 (rather than 40) μM $Fe^{III}$ citrate; *CSM-6.5* and *CSM-6.5 low*, same but using pH 6.5 mobile phase.

Author Manuscript Author Manuscript Author Manuscript Author Manuscript

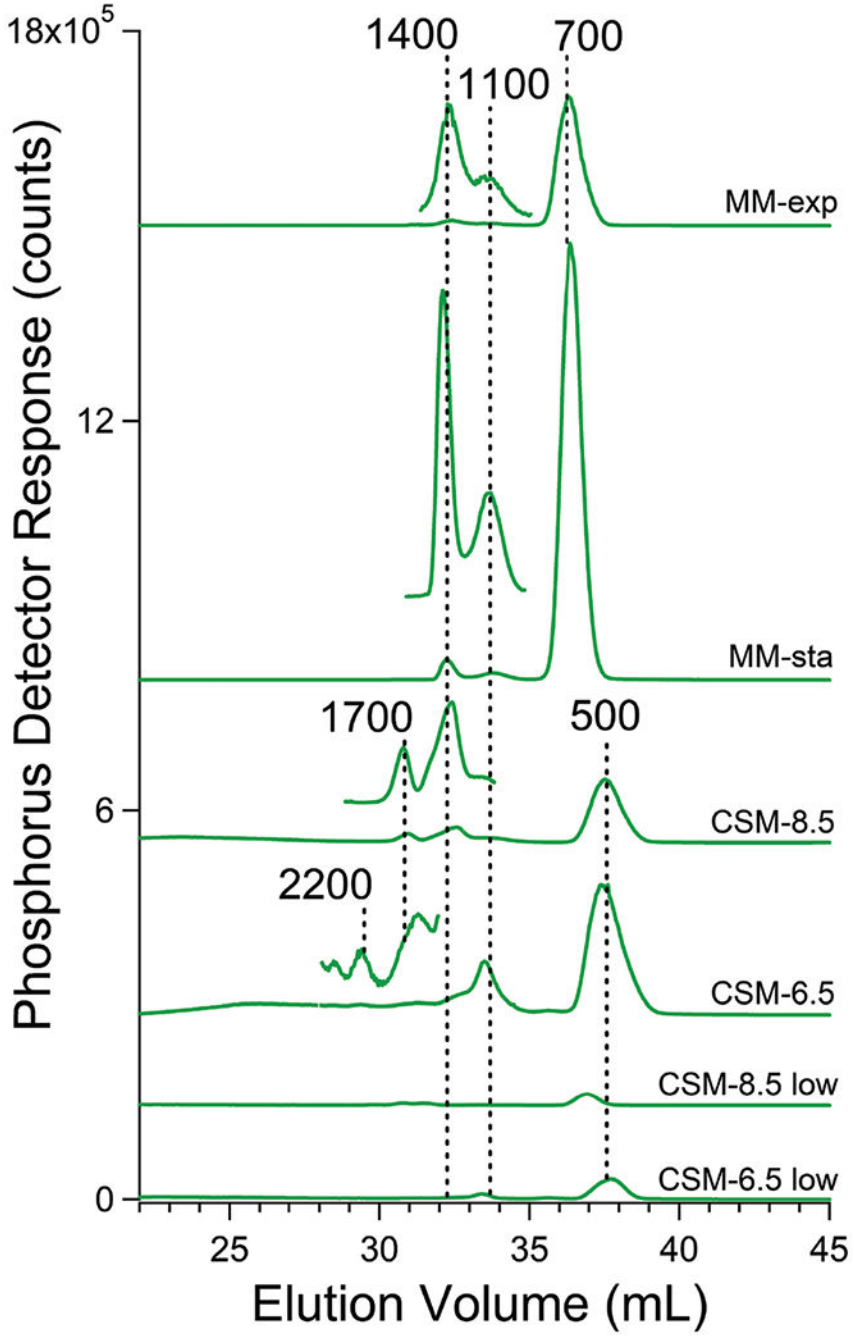


**Fig. 4.**

Averaged phosphorus-detected chromatograms of FTS from isolated vacuoles. Trace labels are as in Fig. 3 legend. Magnification of certain regions of the chromatograms allows easy visualization of low-intensity peaks.

Author Manuscript Author Manuscript Author Manuscript Author Manuscript

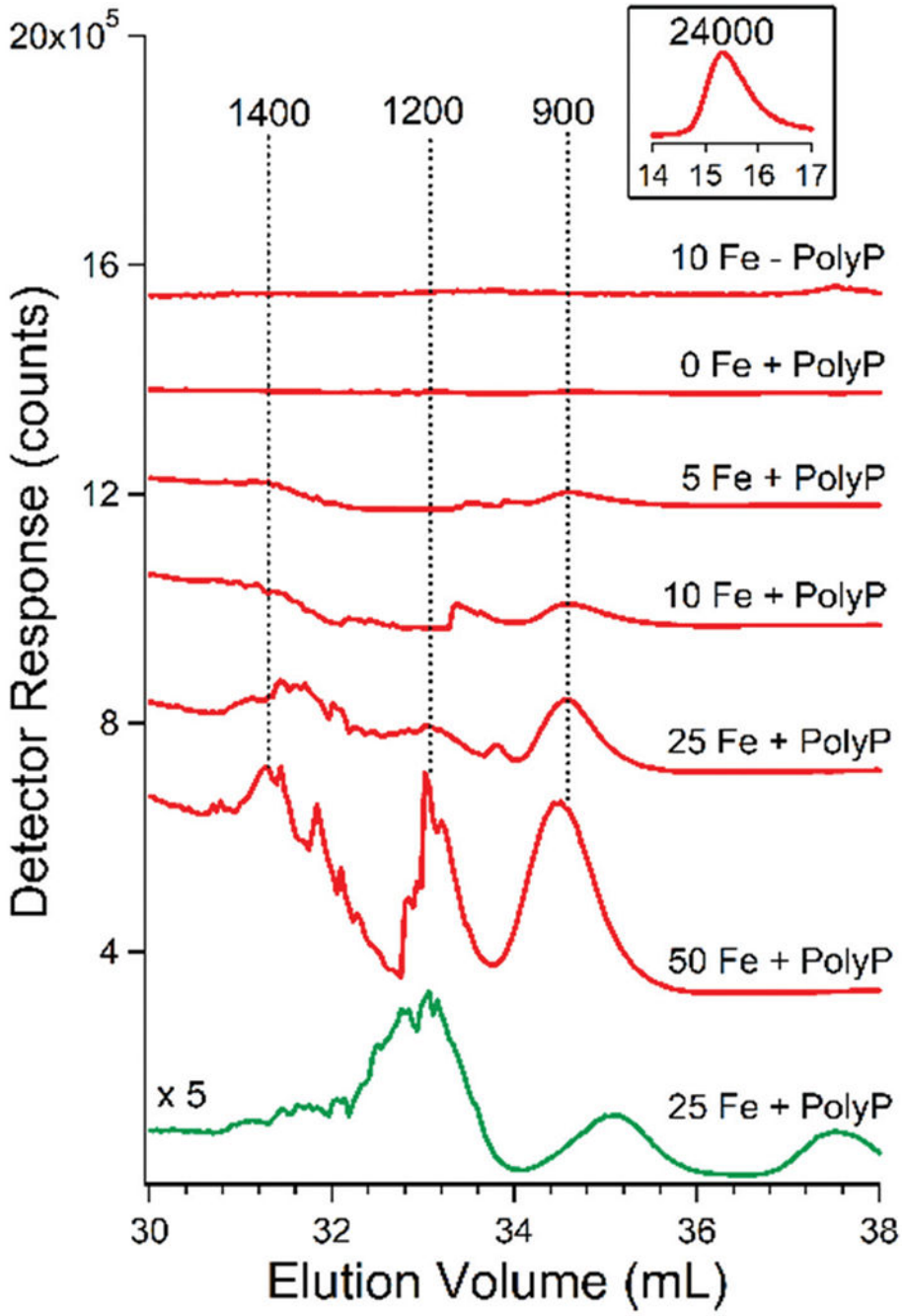


**Fig. 5.**

Chromatography traces of synthetic $Fe^{III}$ polyphosphate. Red traces are Fe, green trace is P. The number before Fe indicates the concentration of $FeCl_3$ in μM used. The concentration of PolyP was 0.5 mg $mL^{-1}$ in all runs. The inset above the top trace is of the same trace but at an earlier elution volume. The pH of the mobile phase was 8.5.

Author Manuscript Author Manuscript Author Manuscript Author Manuscript

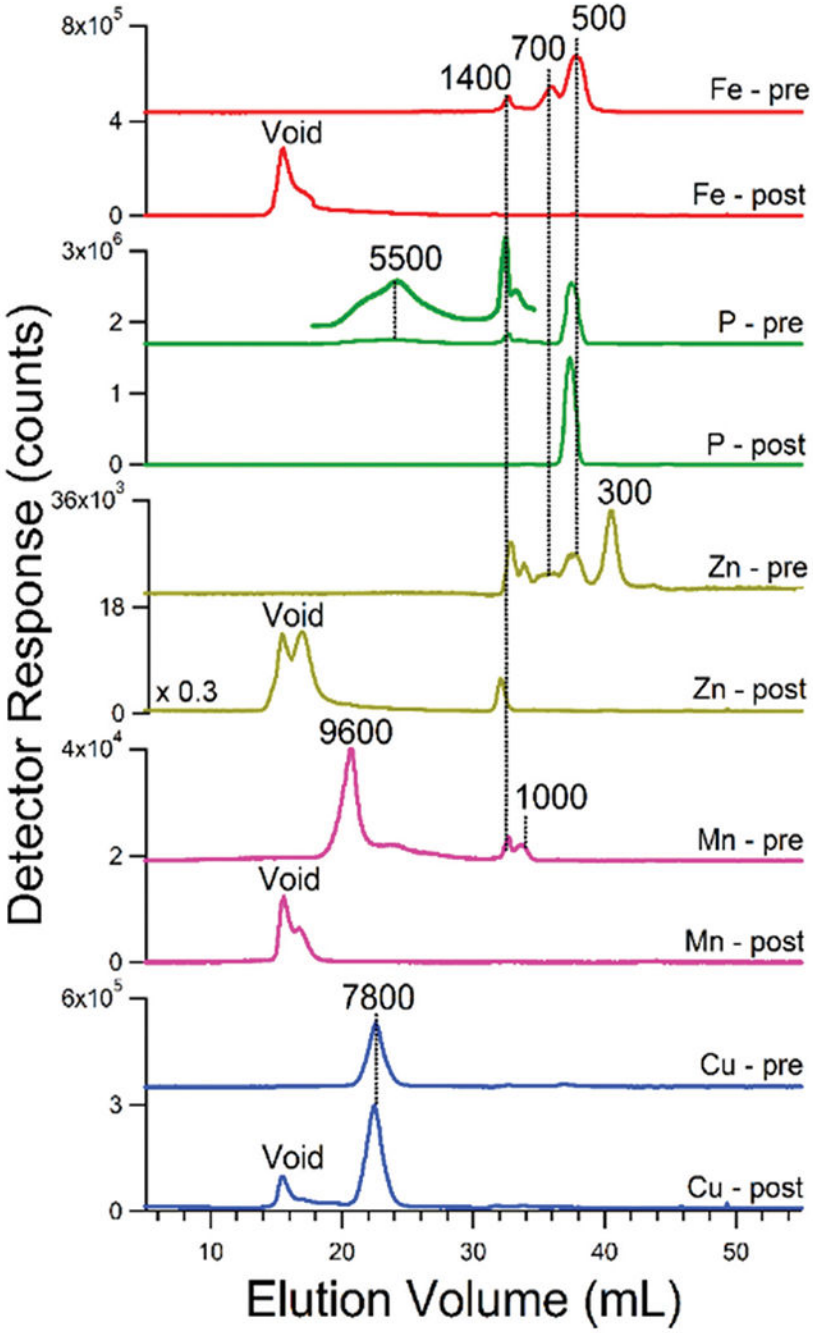


**Fig. 6.**

Effect of acid phosphatase on vacuolar FTS traces of batch 13. Element symbol-*pre*, before treatment; element-symbol-*post*, after treatment. See Experimental procedures for reaction details

Author Manuscript Author Manuscript Author Manuscript Author Manuscript

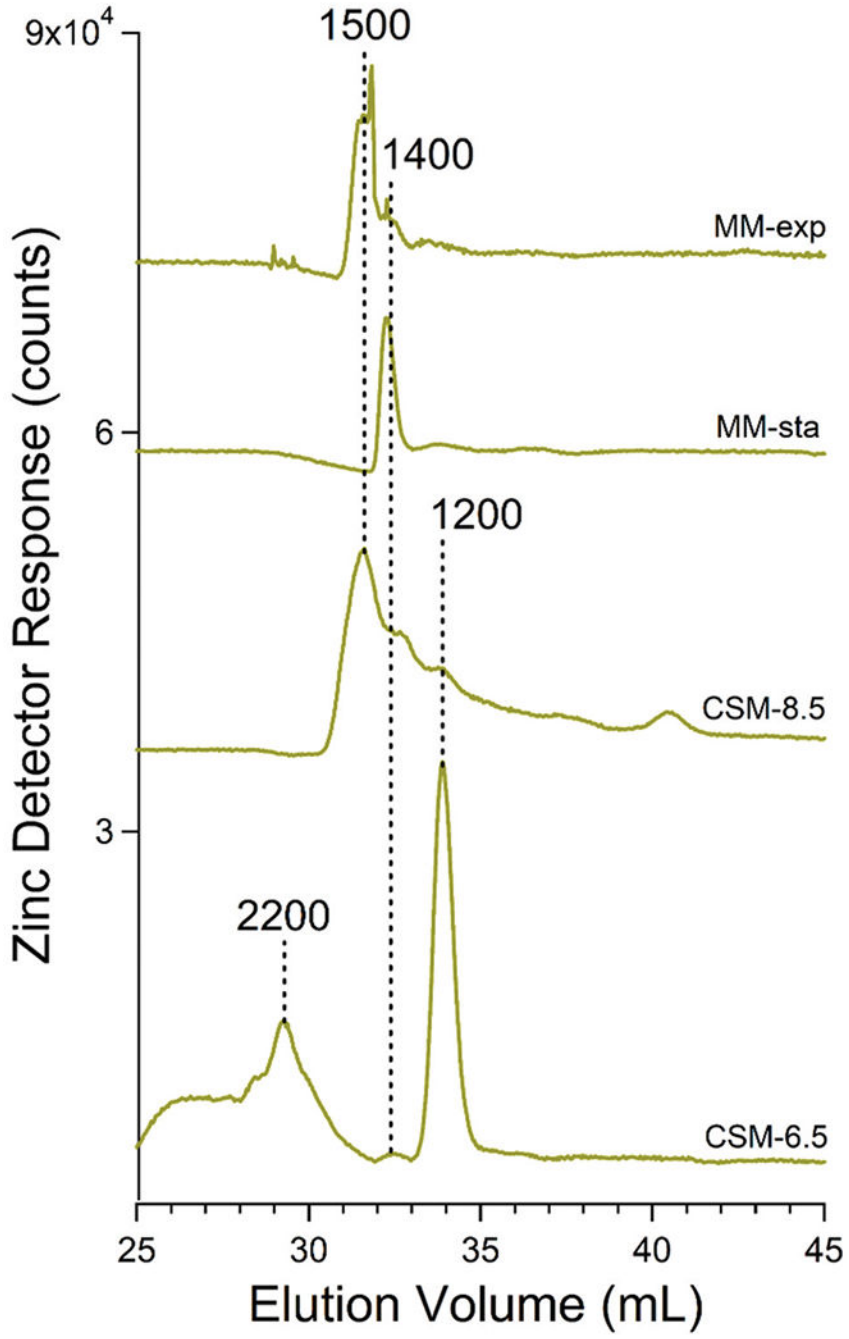


**Fig. 7.**

Averaged zinc-detected chromatograms of FTSs from isolated vacuoles. Trace labels are as in Fig. 3.

Author Manuscript Author Manuscript Author Manuscript Author Manuscript

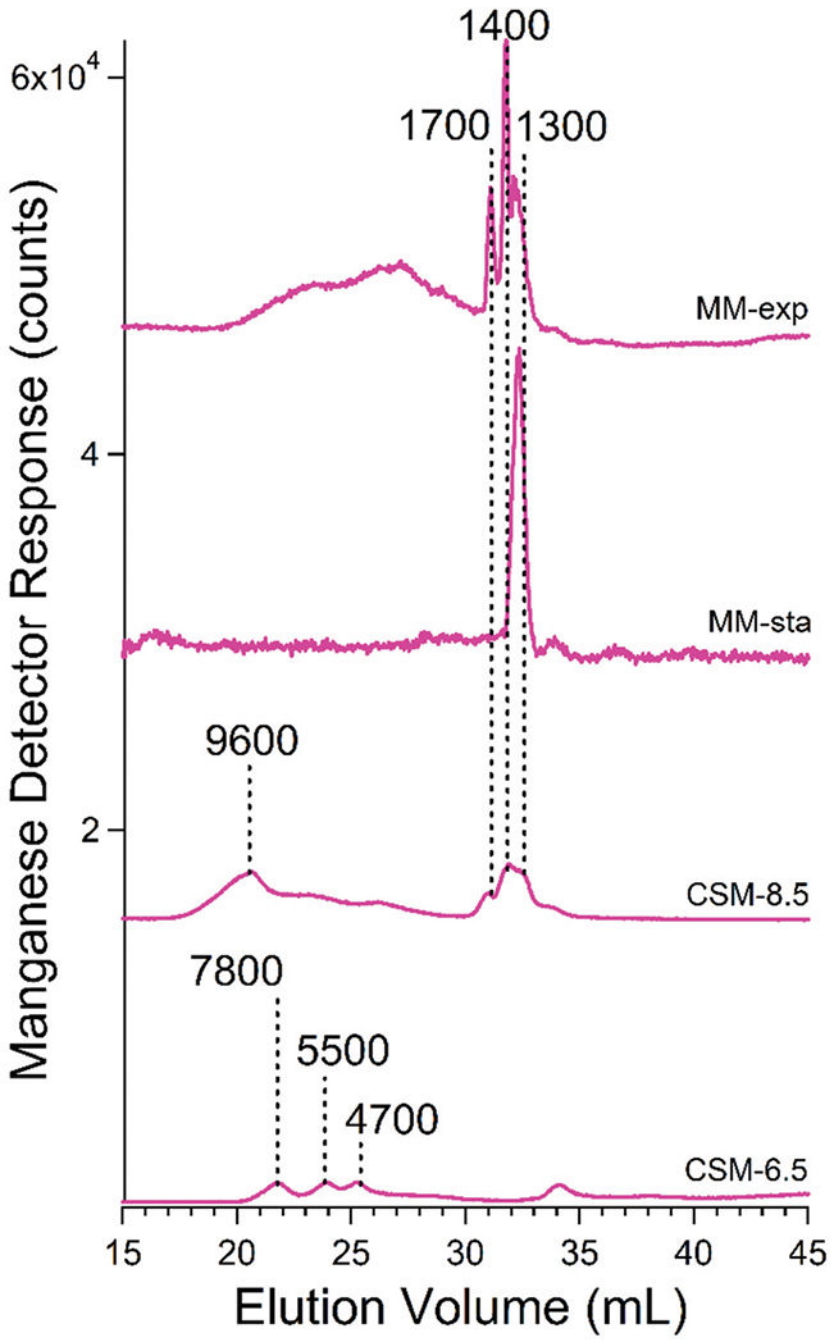


**Fig. 8.**

Averaged manganese-detected chromatograms of FTSs from isolated vacuoles. Trace labels are as in Fig. 3 legend.

Author Manuscript Author Manuscript Author Manuscript Author Manuscript

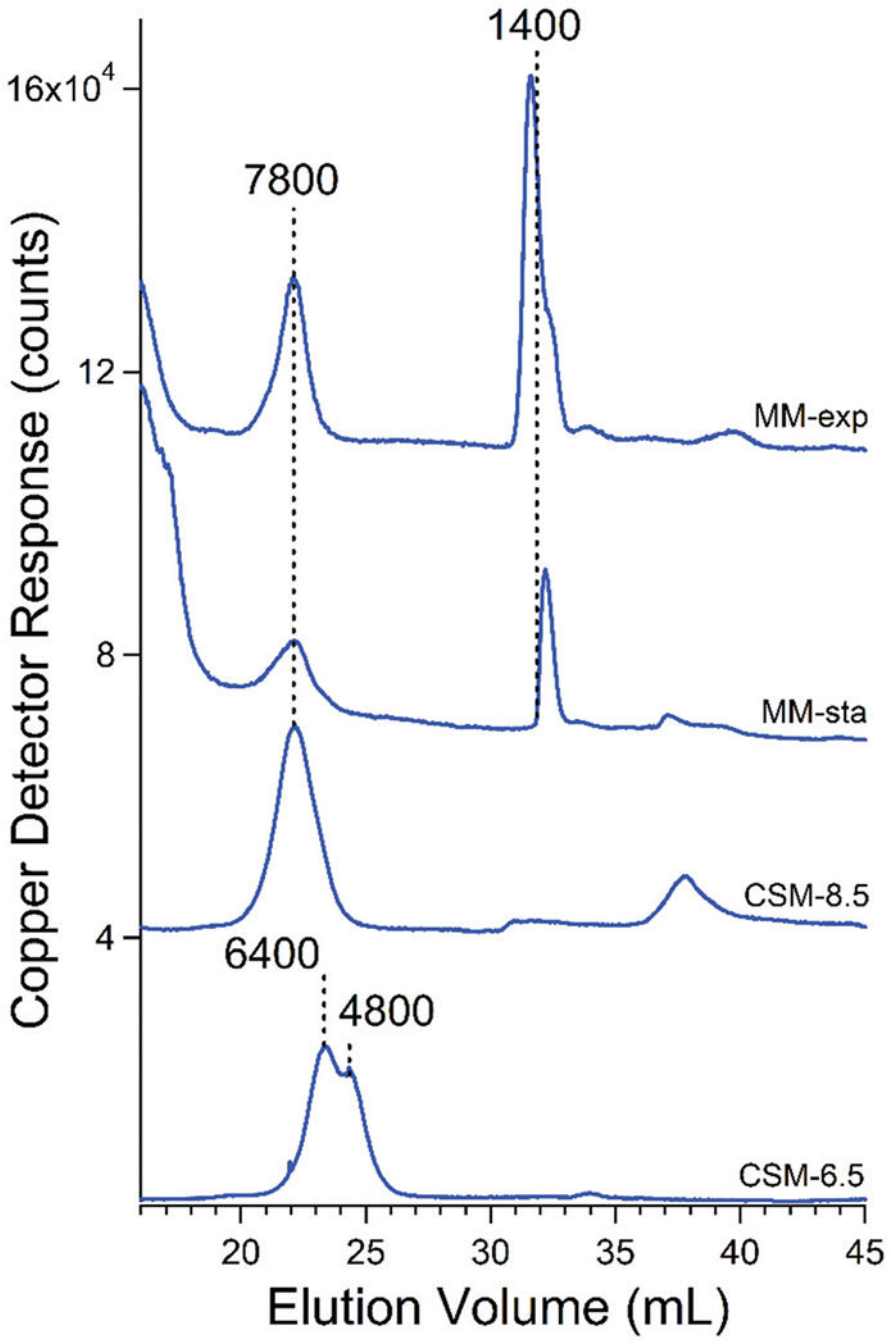


**Fig. 9.**

Averaged copper-detected chromatograms of FTS from isolated vacuoles of WT strain. Trace labels are as in Fig. 3 legend.

Author Manuscript Author Manuscript Author Manuscript Author Manuscript

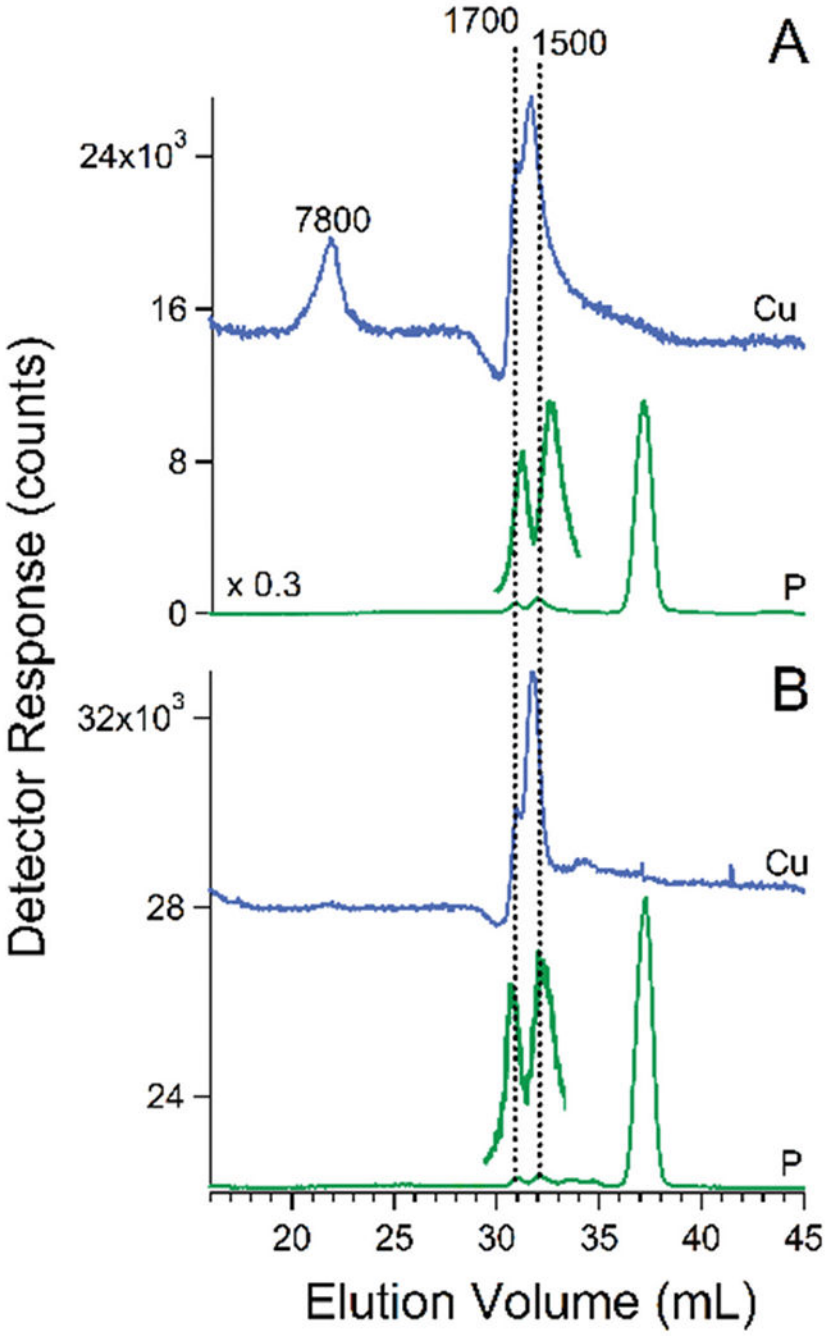


**Fig. 10.**

Copper and phosphorus-detected chromatograms of FTS from isolated vacuoles of *cox17Δ* strain (panel A) and *cup1Δ* strain (panel B). Blue trace is Cu, green trace is P. The pH of the mobile phase was 8.5.

Author Manuscript Author Manuscript Author Manuscript Author Manuscript

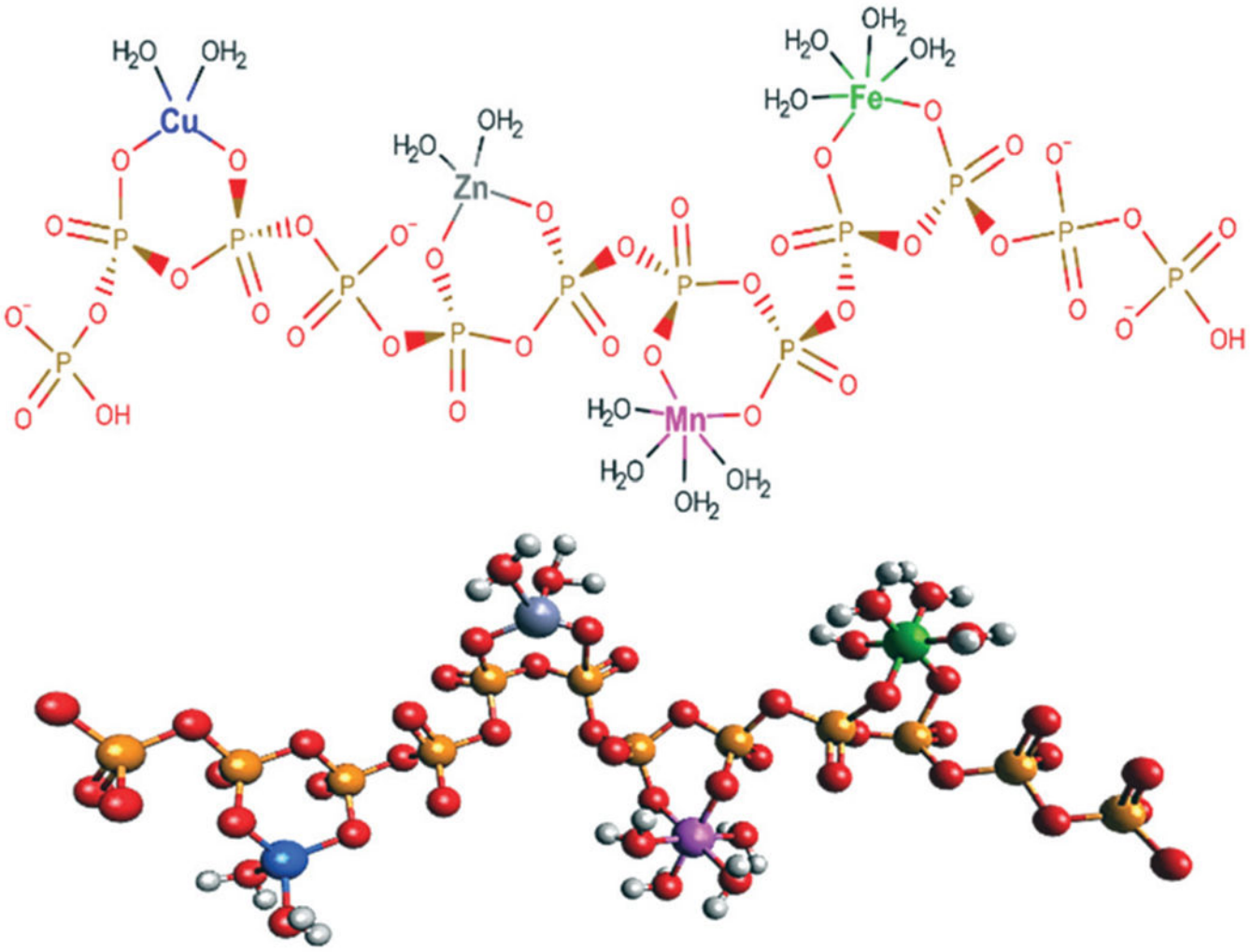


**Fig. 11.**

Hypothetical structure of a $n = 12$ metal:polyphosphate complex with a mass of *ca.* 1400 Da. Metals are presumed to bind as chelates to a floppy chain. It is statistically unlikely that all four metal ions coordinate, as drawn, to a single chain of this length. No particular stereochemistry is implied. 2D and 3D structures were generated using *MarvinSketch* (https://chemaxon.com/products/marvin) and *Avogadro* (https://avogadro.cc/), respectively.